NeuroImage 95 (2014) 208–216

Contents lists available at ScienceDirect

NeuroImage

journal homepage: www.elsevier.com/locate/ynimg

Spatial variability of functional brain networks in early-blind and sighted subjects

Robert Boldt [a,b,c,*], Mika Seppä [a], Sanna Malinen [a], Pia Tikka [d], Riitta Hari [a], Synnöve Carlson [a,b]

[a] Brain Research Unit, O.V. Lounasmaa Laboratory, School of Science, Aalto University, Finland
[b] Neuroscience Unit, Institute of Biomedicine/Physiology, University of Helsinki, Finland
[c] Advanced Magnetic Imaging Centre, Aalto NeuroImaging, School of Science, Aalto University, Finland
[d] Department of Film, Television and Scenography, School of Arts, Design and Architecture, Aalto University, Finland

ARTICLE INFO

Article history:
Accepted 20 March 2014
Available online 27 March 2014

Keywords:
Blindness
fMRI
Independent component analysis
Plasticity
Auditory cortex
Visual cortex

ABSTRACT

To further the understanding how the human brain adapts to early-onset blindness, we searched in early-blind and normally-sighted subjects for functional brain networks showing the most and least spatial variabilities across subjects. We hypothesized that the functional networks compensating for early-onset blindness undergo cortical reorganization. To determine whether reorganization of functional networks affects spatial variability, we used functional magnetic resonance imaging to compare brain networks, derived by independent component analysis, of 7 early-blind and 7 sighted subjects while they rested or listened to an audio drama. In both conditions, the blind compared with sighted subjects showed more spatial variability in a bilateral parietal network (comprising the inferior parietal and angular gyri and precuneus) and in a bilateral auditory network (comprising the superior temporal gyri). In contrast, a vision-related left-hemisphere-lateralized occipital network (comprising the superior, middle and inferior occipital gyri, fusiform and lingual gyri, and the calcarine sulcus) was less variable in blind than sighted subjects. Another visual network and a tactile network were spatially more variable in the blind than sighted subjects in one condition. We contemplate whether our results on inter-subject spatial variability of brain networks are related to experience-dependent brain plasticity, and we suggest that auditory and parietal networks undergo a stronger experience-dependent reorganization in the early-blind than sighted subjects while the opposite is true for the vision-related occipital network.

Introduction

Congenital or early blindness affects the structure and function of the brain (Pascual-Leone et al., 2005). Although knowledge about the neural mechanisms underlying brain plasticity following early blindness is accumulating, a more thorough comprehension of experience-dependent brain plasticity is required and could aid e.g. in the development of sensory substitution devices for the blind. It is thus important to understand how the human brain adapts to missing sensory input. Recent methodological advances have provided new ways to study brain organization and plasticity. One rapidly growing field is the study of functionally-connected brain networks (Calhoun and Adali, 2012), such as the "resting-state networks". Commonly studied resting-state networks include (i) the default-mode network comprising areas within the posterior cingulate and precuneus, the parietal lobes bilaterally, and the medial prefrontal cortex (Raichle et al., 2001), (ii) the motor/sensory network comprising the pre- and postcentral gyri, and the premotor and supplementary motor areas (Biswal et al., 1995), (iii) the vision-related occipital network, and (iv) the superior temporal network covering auditory cortices (Damoiseaux et al., 2006). Topographies of these brain networks are rather similar both during rest and task performance (Smith et al., 2009), although hubs may shift during tasks, suggesting a more efficient information transmission (Di et al., 2013). As blind subjects cannot execute visual tasks, resting-state studies could be helpful in unraveling the functional connectivity of visual areas.

Early-blind subjects can have improved auditory and tactile abilities or maladjustments in senses other than vision. These two types of alterations are addressed by the compensatory-plasticity hypothesis and the general-loss hypothesis, respectively (Pascual-Leone et al., 2005). Early-blind subjects often perform better than sighted subjects in auditory (Gougoux et al., 2004, 2005) and tactile tasks (Goldreich and Kanics, 2003; Wan et al., 2010), which lends support to the compensatory-plasticity hypothesis. On the other hand, the general-loss hypothesis is supported by findings that blind subjects perform poorly in auditory localization tasks that seem to benefit from intact vision (Gori et al., 2014; Zwiers et al., 2001) and in tasks requiring auditory–tactile interaction in the peripersonal space (Collignon et al., 2009).

* Corresponding author at: PO BOX 15100, 00076 Aalto, Finland. Fax: +358 9 19125302.
E-mail address: robert.boldt@helsinki.fi (R. Boldt).

http://dx.doi.org/10.1016/j.neuroimage.2014.03.058

Resting-state functional magnetic resonance imaging (fMRI) studies comparing early-blind with sighted subjects show reduced functional connectivity—in accordance with the general-loss hypothesis—within occipital areas and within a wide network extending from occipital to parietal somatosensory, frontal motor, and temporal multisensory areas (Yu et al., 2008). On the other hand, functional connectivity between visual and language areas is enhanced in anophthalmic (Watkins et al., 2012) and early-blind subjects, supporting the compensatory-plasticity hypothesis (Liu et al., 2007).

The structure and function of resting-state networks, such as the default-mode network and language-related networks, are in part genetically determined (Glahn et al., 2010; Jamadar et al., 2013). Environmental influences and experience, including practice (Jang et al., 2011) and disease (Greicius et al., 2004), however, induce changes in these networks. Accordingly, the investigation of variability in functional networks provides one approach to explore how experience, including early blindness, affects the brain (Lee et al., 2012; Liu et al., 2007; Mueller et al., 2013). Importantly, individual variability should not be considered noise, but rather as an essential feature helping to understand how the brain matures (Zilles and Amunts, 2013). Therefore, it is conceivable that sensory loss may affect brain structure and function in a variable manner and result in increased individual variability of functional brain networks.

We hypothesized that experience-dependent brain plasticity is reflected in inter-subject spatial variability of functional networks. In line with this hypothesis, the brain regions of children communicate locally with other regions, but with increasing age communication becomes more distributed as a result of experience-dependent processes (Fair et al., 2009; Satterthwaite et al., 2013). We explored whether the networks compensating for early-onset visual deprivation would exhibit more inter-subject spatial variability in the early-blind than sighted subjects. We also investigated whether some of the networks that are little used after early-onset visual deprivation, e.g. occipital networks devoid of visual input, would exhibit less inter-subject spatial variability in the blind than the sighted subjects. We estimated functional networks with independent component analysis (ICA) that, in contrast to seed-based correlation analysis, requires no anatomical seed regions and can reliably reveal comparable intrinsic and task-related connectivity patterns (Smith et al., 2009), despite coactivation of distinct networks during tasks (Joel et al., 2011). Thus ICA allowed us to compare the functional networks found in the data collected during rest and audio-drama listening. We also searched for possible between-group differences in functional network connectivity (Jafri et al., 2008) in the networks displaying large spatial variability between the blind and sighted subjects.

We analyzed both resting-state data and data collected while the subjects listened to an audio drama. In line with our hypothesis, the functional networks showing more variability in the blind than the sighted subjects encompassed auditory, parietal, and sensorimotor areas, i.e. regions that are modulated by altered sensory experience due to early-onset blindness. One network that encompassed visual occipital areas was less variable in the blind than sighted subjects.

Methods

Subjects

Seven early-blind subjects (4 females, 3 males; age range 19–43 years, mean age 34 years; 6 right-handed and one ambidextrous by report; see Table 1 for the causes and durations of the blindness) and 16 normally-sighted subjects (7 females, 9 males; age range 19–37 years; mean age 24 years, all right-handed by report) with no recorded history of neurological or psychiatric problems participated in the experiment; the data of 13 normally-sighted subjects were obtained from our previous study (Boldt et al., 2013). All blind subjects read Braille (mean ± SD 4.9 ± 2.6 h/week; range 2–8). For the main analysis, an age- and gender-matched control group (4 females, 3 males; age range 19–37 years, mean age 27 years) was formed of the sighted subjects; the data of the remaining 9 normally-sighted subjects were only used for creating a reference distribution (see Creating a reference distribution section). The subjects were native Finns and fluent in Finnish although one blind and one sighted subject included in the main analysis were Swedish-speaking bilinguals. The subjects participated after informed consent, and the study was approved by the ethics committee of the Helsinki and Uusimaa Hospital District.

Data acquisition and preprocessing

MRI data were obtained with a Signa VH/i 3.0 T MRI scanner (General Electric, Milwaukee, WI, USA). First, a structural image of 178 axial slices was acquired using a T1-weighted 3D-MPRAGE-sequence, TR = 10 ms, TE = 30 ms, preparation time = 300 ms, flip angle = 15°, FOV = 25.6 cm, matrix = 256 × 256, and voxel size = 1 × 1 × 1 mm^3. Next, functional images were acquired using a gradient echo-planar-imaging sequence with the following parameters: TR = 2.5 s, TE = 30 ms, flip angle = 75°, FOV = 22.0 cm, matrix = 64 × 64, slice thickness = 3.5 mm, voxel size = 3.4 × 3.4 × 3.5 mm^3 and number of oblique axial slices = 43. Slices were obtained using interleaved acquisition. Altogether 246 functional volumes were collected, but the first 6 dummy volumes were automatically discarded. The resting-state scan lasted about 10 min. Subjects were instructed to lie still with their eyes closed, not to fall asleep and not to think of anything in particular. After the resting-state scan, an audio drama was presented (Boldt et al., 2013). The functional images during the audio drama were acquired using the same parameters as in the resting-state scan, but the scan lasted about 19 min resulting in 456 functional volumes. We refer to this set of data as the audio-drama data.

As described in detail in our previous study of normally-sighted subjects (Boldt et al., 2013), the audio drama comprised sequences from a Finnish movie "Postia Pappi Jaakobille" ("Letters to Father Jaakob", director Klaus Härö, Production company: Kinotar Oy, Finland, 2009), in which a woman arrives at a run-down parsonage to help an old blind priest. The stimulus included sounds from the original movie, and a narration for blind people. The audio drama was presented binaurally with UNIDES ADU2a audio system (Unides Design, Helsinki, Finland) from a

Table 1
Characteristics of the early-blind subjects.

Gender	Age (years)	Age when blind	Cause of blindness
M	36	Since birth	Norrie's disease, no other neurological deficits
F	36	Since 3 years of age	Cataract, aniridia
F	19	Since birth	Leber's congenital amaurosis
F	40	Since birth	Leber optic atrophy
F	39	Since 6 months of age	Retinopathy of prematurity
M	43	Shadows and light until the age of 3 years	Retinopathy of prematurity
M	27	Since birth	Retinopathy of prematurity

F = female, M = male.

PC with an audio amplifier (Denon AVR-1802) and a power amplifier (Lab.gruppen iP 900). Sounds were delivered to the subject through plastic tubes connected to earplugs (Etymotic Research, ER3, IL, USA) that were inserted into the ear canals. The subject wore earmuffs to dampen the background noise of the magnet. Before scanning, we played parts of the audio-drama introduction to the subjects to adjust the sound level. The sound level was gradually raised until the sound level was loud but still comfortable. Subjects were instructed to lie still with their eyes closed and to listen attentively to the audio drama.

For independent component analysis (see below, Independent component analysis section), volume data were preprocessed using FS-FAST pipeline of FreeSurfer v5.1.0 software (http://surfer.nmr.mgh.harvard.edu/) by including registration of the functional images to the anatomical images, motion correction, slice-timing correction, intensity normalization, normalization into 2-mm MNI space, and spatial smoothing with a 12-mm full-width-at-half-maximum Gaussian kernel. To adequately estimate independent components in most of the subjects, we used a large smoothing kernel as suggested previously (Allen et al., 2012). The resting-state data and the first 240 functional volumes collected while subjects listened to the audio drama were preprocessed independently, but with identical parameters.

Independent component analysis

We used group ICA toolbox GIFT v1.3 (http://icatb.sourceforge.net/) to estimate the independent components (ICs) corresponding to the functional networks. The 7 blind and 7 age- and gender-matched sighted subjects were grouped together for the analysis. Group ICA seeks ICs for the group data instead of estimating networks separately for each individual. We chose this approach to avoid the ambiguity arising from combining the different individual networks resulting from separate estimations. The minimum-description-length algorithm (Li et al., 2007) implemented in GIFT estimated the mean number of sources to be 53. Spatial networks were determined using the Infomax algorithm (Lee et al., 1999). The ICASSO method (Himberg et al., 2004) was used to assess the replicability of the networks by running the algorithm 100 times; the most representative networks of estimated clusters were selected. Back-reconstruction of individual networks and time-courses was done with the GICA3 algorithm (Erhardt et al., 2011). Resulting spatial networks were scaled to percent signal change to maximize sensitivity to regional differences (Allen et al., 2012). Group ICA was run independently, but with identical parameters for the resting-state data and the first 240 functional volumes collected while subjects listened to the audio drama.

We identified functional networks located in the gray matter (Stevens et al., 2007). Functional networks (thresholded at family-wise error (FWE)-corrected $p < 0.05$, $t > 8.62$) that had >67% overlap with binarized gray-matter MNI-template (SPM8) were considered physiologically plausible and were thus retained for further analysis.

Correlating networks within subjects and between groups

Our main aim was to determine whether the intra-group spatial variability of the functional networks would differ between the groups of blind and sighted subjects. We assumed that experience-related modulation of certain brain areas would increase inter-individual spatial variability, and hence the functional networks compensating for early-onset blindness would be inter-individually less correlated in the blind than sighted subjects, whereas the functional networks that are used less following early-onset blindness would show the opposite effect. Thus, we analyzed the data to find out whether any of the functional networks in the group of early-blind subjects had a mean between subjects correlation that was different from the respective correlation in the sighted group. We measured how similarly the voxels of a functional network were distributed throughout the brain, both between subjects within the groups, and between the groups, by computing pairwise Pearson's correlations for the individual, unthresholded spatial gray-matter network maps, between all pairs of subjects, separately within each group. Next, the within-group pairwise correlation values were compared between the groups with a Mann–Whitney test. This procedure resulted in a U-value, which was compared with a reference distribution (see Creating a reference distribution section) to estimate the statistical significance (p-value). We carried out the analysis identically but independently for the resting-state data and the audio-drama data. Fig. 1 depicts the method.

To find the group resting-state networks corresponding to the group networks derived from the audio-drama data, we used the spatial correlation function available in the GIFT toolbox and searched for the highest spatial correlations between the resting-state networks and the networks derived from the audio-drama data.

Creating a reference distribution

We estimated a reference distribution from the sighted subjects' data to avoid possible confounds that could result from the statistical dependence of the pairwise correlation (Kim et al., 2008) and the back-reconstruction step performed to obtain individual networks. We estimated the reference distribution using all 16 normally-sighted subjects, which included the 7 subjects used in the blind-versus-sighted comparison. A sample of 14 subjects was taken without replacement from the 16 normally-sighted subjects. The subjects were randomly divided into two groups of 7 in each. ICA was run for the sample with the same parameters as in the blind-versus-sighted comparison. Inter-subject correlation for all pairwise comparisons was calculated for each network in both groups. The resulting pairwise correlation values were compared between the groups with a Mann–Whitney test. The process was repeated for all 120 possible

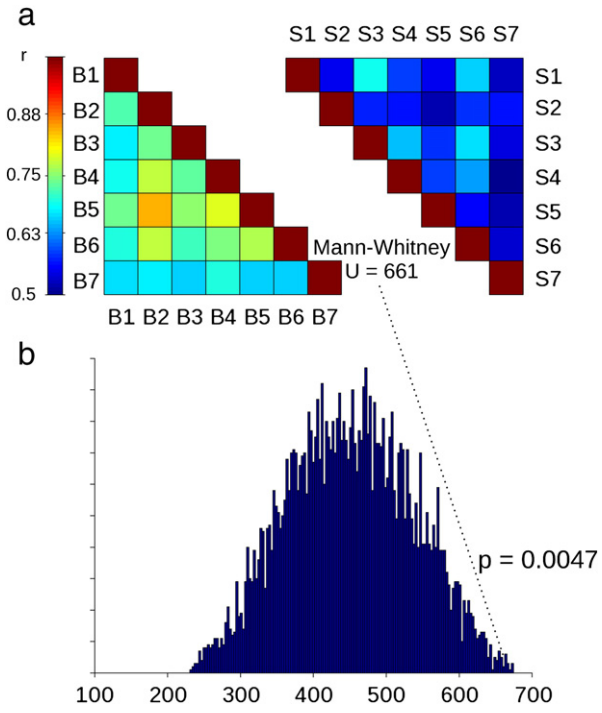

Fig. 1. Illustration of how the difference in functional network variability was measured between the groups, here using IC25r as an example. a) For each ICA-derived functional network, pairwise Pearson's correlations (r) were computed for the individual unthresholded functional networks between all pairs of subjects, separately within the blind (B) and sighted (S). This computation resulted in 21 pairwise comparisons in each group. Next, the within-group pairwise correlation values were compared between the groups with a Mann–Whitney test which resulted in a U-value. b) A reference distribution, sampled from the data of 16 sighted subjects (see Creating a reference distribution), was used to estimate the tail probability (i.e. p-value) for this U-value.

combinations obtained by selecting 14 subjects out of 16. Employing all 53 networks, a total of 53 * 120 = 6360 values were obtained to estimate the reference distribution. We used the frequencies of the values in the reference distribution to compute p-values for each network in the two-tailed tests between the blind and sighted subjects, and the p-values were corrected for false discovery rate (FDR).

Functional network connectivity

We searched for functional network connectivity for networks that displayed statistically significant between-group differences in spatial variability. Within each subject, we first correlated the time-courses of these networks with the functional networks that displayed no significant differences in variability between the groups (Jafri et al., 2008). The resulting correlation values were Fisher-transformed, after which we tested the correlation values against zero (one-sample t-test; DOF = 6), separately for the two subject groups, blind and sighted. We then tested the statistical significance of group differences in functional network connectivity (two-sample t-test; DOF = 12; Bonferroni correction for multiple comparisons).

Results

Networks during rest

Of the 53 networks estimated from the data collected during rest, 25 were classified as gray-matter networks and thus suitable for further analysis. Supplementary Fig. S1 depicts these networks ordered so that the network that displayed the largest variability among the blind compared with the sighted subjects (IC1r) is shown first and the network with the least variability (IC25r) is shown last. Each network had a quality index >0.9 (on a scale from 0 to 1) (Himberg et al., 2004), indicating reasonable reliability of the estimated networks. From the 25 networks, four (IC1r, IC2r, IC3r, and IC25r) displayed statistically significantly different spatial variability between the groups (FDR corrected threshold, $p < 0.0083$).

Fig. 2 shows the three networks (IC1r, IC2r, and IC3r; blue frame in Fig. 2 and Supplementary Fig. S1) that were significantly more variable in the blind than the sighted subjects: (1) IC1r, "a parietal network", comprised bilaterally the angular and inferior parietal gyri, and the left precuneus; the within-subject correlation values differed between the blind and sighted subjects ($r_{blind} = 0.58$, $r_{sighted} = 0.68$; $p = 0.0006$). (2) IC2r, "an auditory network", comprised the superior temporal and Heschl's gyri extending to the postcentral and supramarginal gyri, Rolandic operculum, and insula of both hemispheres ($r_{blind} = 0.64$, $r_{sighted} = 0.72$; $p = 0.0016$). (3) IC3r, "a tactile network", encompassed bilaterally the postcentral gyrus and extended in the right hemisphere to the precentral gyrus ($r_{blind} = 0.55$, $r_{sighted} = 0.71$; $p = 0.0022$). Moreover, Fig. 2 shows network IC25r (brown frame in Fig. 2 and in Supplementary Fig. S1) that was significantly less variable among the blind than sighted subjects. This "visual network" encompassed the left superior, middle, and inferior occipital gyri and the fusiform, lingual and calcarine sulcus ($r_{blind} = 0.72$, $r_{sighted} = 0.58$; $p = 0.0047$). Table 2 shows a list of areas encompassed by all 25 networks displayed in Supplementary Fig. S1.

Networks during audio drama

Of the 53 estimated networks that were related to the audio drama, 24—an amount similar to the 25 resting-state gray-matter networks—were classified as gray-matter networks. Supplementary Fig. S2 depicts these networks ordered so that the network that displayed the largest

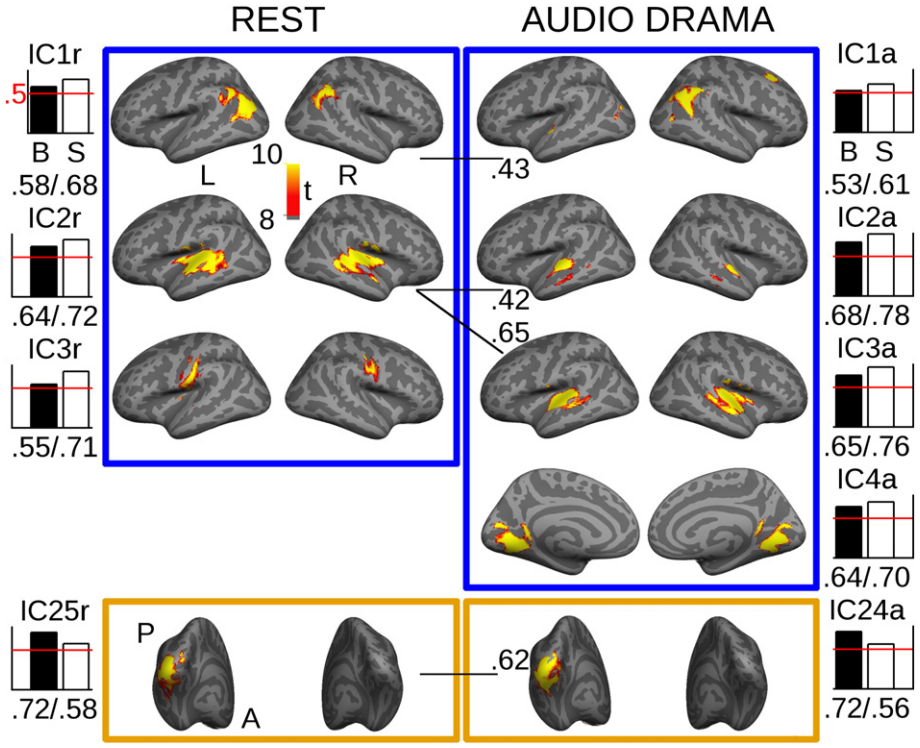

Fig. 2. Functional networks (groups combined) that were statistically significantly more (blue frames) or less (brown frames) variable among the blind than sighted subjects during rest (IC1r, IC2r, IC3r and IC25r), or during listening to an audio drama (IC1a, IC2a, IC3a, IC4a and IC24a). The bars show the mean correlation values for the blind (B; black bars) and sighted (S; white bars) groups for each network; the values are also indicated below the bars, the horizontal red line is set at r = 0.5. Three networks (IC1r, IC2r, and IC3r) were more variable among the blind than sighted subjects during rest and four networks (IC1a, IC2a, IC3a, and IC4a) more variable while subjects listened to an audio drama. One network was less variable among the blind than sighted subjects during rest (IC25r) and one (IC24a) while subjects listened to an audio drama. The black lines link resting-state networks with spatially matching audio-drama networks. The networks are thresholded (FWE-corrected $p < 0.05$, cluster size > 100 voxels) for illustrative purposes although the variability was measured with pair wise correlations of the unthresholded spatial maps. L = left, R = right, A = anterior, P = posterior.

Table 2
Peak voxel coordinates (x, y, and z in MNI system) and anatomical labels for the resting-state networks.

IC #	x	y	z	Region	N
1r	−46	−65	35	Angular gyrus, inferior parietal gyrus	2271
	60	−57	43	Angular gyrus, inferior parietal gyrus	1075
	−12	−49	33	Precuneus	124
2r	−54	−9	11	Superior temporal gyrus, postcentral gyrus, Rolandic operculum, supramarginal gyrus, insula, Heschl's gyrus, middle temporal gyrus	3552
	42	−7	19	Superior temporal gyrus, postcentral gyrus, Rolandic operculum, supramarginal gyrus, insula, Heschl's gyrus	3459
3r	−66	−17	37	Postcentral gyrus	1221
	46	−15	53	Postcentral gyrus, precentral gyrus	639
4r	−22	−81	33	Superior and middle occipital gyri, angular gyrus, superior and inferior parietal gyri	3346
	28	−89	33	Superior and middle occipital gyri, angular gyrus, superior parietal gyrus, cuneus	2026
	−22	−43	−11	Fusiform gyrus	117
	4	−55	15	Precuneus	291
5r	44	49	1	Triangular and opercular part of inferior frontal gyrus, middle frontal gyrus, precentral gyrus	5265
6r	−52	13	31	Triangular, opercular and orbital part of inferior frontal gyrus, middle frontal gyrus, precentral gyrus, Rolandic operculum	5555
	48	35	13	Triangular part of inferior frontal gyrus, middle frontal gyrus	114
	−54	−45	47	Inferior parietal gyrus	314
7r	−4	−7	27	Bilaterally anterior and middle cingulate, medial part of superior frontal gyrus	3490
8r	−2	−39	43	Bilaterally precuneus, median cingulate gyrus and paracentral lobule, right supplementary motor areas	3301
9r	8	−55	−47	Cerebellum	2787
10r	−18	55	27	Bilaterally middle frontal gyrus, superior frontal gyrus, left middle cingulate gyrus	5032
11r	58	−33	11	Middle and superior temporal gyri, angular gyrus	2768
12r	−8	−71	27	Bilaterally precuneus, cuneus, median and posterior cingulate gyri, calcarine sulcus	5840
	−46	−67	33	Angular gyrus	271
	8	−17	5	Thalamus	144
13r	42	−81	19	Angular gyrus, inferior and superior parietal gyri, superior and middle occipital gyri, precuneus	3936
	36	7	55	Middle frontal gyrus	266
14r	−8	−71	24	Bilaterally precuneus, left cuneus	1128
15r	−26	−71	53	Superior and inferior parietal gyri, angular gyrus, superior and middle occipital gyri	3869
	32	−61	51	Superior parietal gyrus	132
16r	6	43	−3	Bilaterally anterior cingulate gyrus and medial part of superior frontal gyrus, left caudate, right middle part of orbital frontal gyrus	3693
17r	−50	13	1	Orbital, triangular and opercular part of inferior frontal gyrus, insula	1792
	46	23	−17	Orbital, triangular and opercular part of inferior frontal gyrus, insula, Rolandic operculum, superior part of temporal pole	2592
18r	−24	−39	69	Postcentral gyrus	100
	26	−59	73	Superior parietal gyrus	118
19r	−20	−99	−5	Cerebellum, lingual gyrus, fusiform gyrus	1385
20r	10	−47	5	Bilaterally calcarine sulcus, lingual gyrus, precuneus, cuneus, vermis	6078
21r	−48	−45	29	Middle and superior temporal gyri, supramarginal gyrus, angular gyrus	2521
	58	−53	17	Superior temporal gyrus	113
22r	0	21	19	Bilaterally medial part of superior frontal gyrus, anterior cingulate gyrus, frontal superior gyrus	3853
23r	14	−85	5	Calcarine sulcus, cuneus, lingual gyrus, superior occipital gyrus	3409
24r	14	−75	11	Bilaterally cuneus, calcarine sulcus and superior occipital gyrus	1707
25r	−56	−69	−11	Superior, middle and inferior occipital gyri, fusiform gyrus, lingual gyrus, cerebellum, calcarine sulcus, inferior temporal gyrus	4473

N refers to the number of voxels in each cluster. Anatomical labeling is based on the group data, and was performed with the Automated Anatomical Labeling (AAL) tool. Labels are listed if a cluster extended ≥100 voxels into the AAL defined area. Threshold $t > 8.62$, FWE-corrected $p < 0.05$, and cluster size > 100 voxels.

variability among the blind compared with the sighted is shown first (IC1a), and the network with the least variability is shown last (IC24a); the networks had a quality index >0.9, except IC16a (0.82) and IC20a (0.80).

From the 24 networks five (IC1a, IC2a, IC3a, IC4a, and IC24a) displayed significantly different spatial variability between the groups (FDR corrected $p < 0.0104$). Fig. 2 shows the four audio-drama networks (IC1a, IC2a, IC3a, and IC4a; blue frame in Fig. 2 and in Supplementary Fig. S2) that were significantly more variable in the blind than sighted subjects: (1) IC1a, a "parietal network", was similar to IC1r, but comprised the inferior parietal gyrus only in the right hemisphere, and displayed some modest clusters in the right middle temporal and middle frontal gyri, and in the left Rolandic operculum. IC1a was significantly more variable in the blind than sighted subjects (mean correlation values: $r_{blind} = 0.53$ and $r_{sighted} = 0.61$, $p < 0.0006$). (2) IC2a, an "auditory network", was found bilaterally in the superior temporal gyrus ($r_{blind} = 0.68$, $r_{sighted} = 0.78$, $p = 0.0006$). (3) IC3a, another "auditory network", encompassed bilaterally the same areas as IC2r, with the exception of that it lacked a left middle temporal gyrus cluster ($r_{blind} = 0.65$, $r_{sighted} = 0.76$, $p = 0.0016$). (4) IC4a, "a visual network", encompassed bilaterally the calcarine sulcus and lingual gyri, precuneus, and cuneus ($r_{blind} = 0.64$, $r_{sighted} = 0.70$, $p = 0.0028$). Moreover, Fig. 2 shows another "visual network" (IC24a; brown frame in Fig. 2 and in Supplementary Fig. S2), lateral and posterior to IC4a, which was significantly less variable among the blind than the sighted, and encompassed the same areas as IC25r, but extended to the cuneus and lacked the inferior temporal gyrus voxels ($r_{blind} = 0.72$, $r_{sighted} = 0.56$, $p = 0.0009$). Table 3 shows a list of the areas encompassed by all 24 networks displayed in Supplementary Fig. S2.

Correspondence between resting-state and audio-drama networks displaying significant variability differences between the groups in both conditions

Fig. 2 shows, for both the resting-state and audio-drama data, the networks that were the most discriminating between the subject groups. Resting-state network IC1r was possibly split during audio drama into networks IC1a and IC16a (not shown in Fig. 2)—correlations 0.43 and 0.43, respectively; the resting-state network IC2r into audio-drama networks IC2a and IC3a (correlations 0.42 and 0.65, respectively). Resting-state network IC25r corresponded to IC24a ($r = 0.62$), resting-state network IC3r corresponded to audio-drama network IC7a ($r = 0.63$), and audio-drama network IC4a corresponded to IC20r ($r = 0.65$). In the following we focus only on the most correlated pairs of networks that displayed significant variability between the blind and sighted subjects during both conditions; the IC1r–IC1a, IC2r–IC3a and IC25r–IC24a pairs. The lines in Fig. 2 link matching networks. Comparison of the resting-state and audio-drama networks implied that two networks, a parietal network (IC1r/IC1a) and an auditory network (IC2r/IC3a), were more variable and a visual network (IC25r/IC24a) less variable in the blind than sighted subjects both during rest

Table 3
Peak voxel coordinates (x, y, and z in MNI system) and anatomical labels for the networks found while subjects listened to an audio drama.

IC #	x	y	z	Region	N
1a	−56	−71	25	Angular gyrus, middle occipital gyrus	522
	62	−67	21	Angular gyrus, inferior parietal gyrus, middle temporal gyrus	2233
	−56	−5	9	Rolandic operculum	173
	26	23	53	Superior and middle frontal gyri	246
	0	−63	35	Bilaterally precuneus	162
2a	−68	−17	9	Superior and middle temporal gyri, postcentral gyrus	1458
	64	−11	9	Superior temporal gyrus	595
3a	−58	−9	11	Superior temporal gyrus, postcentral gyrus, Rolandic operculum, supramarginal gyrus, insula, Heschl's gyrus	2150
	52	−3	13	Superior temporal gyrus, postcentral gyrus, Rolandic operculum, supramarginal gyrus, insula, Heschl's gyrus	3042
4a	0	−45	9	Bilaterally calcarine sulcus, lingual gyrus, precuneus, cuneus, vermis	5746
5a	54	−51	39	Middle and superior temporal gyri, angular gyrus, supramarginal gyrus	4523
	54	−13	39	Precentral gyrus	235
	4	−59	45	Right precuneus	180
6a	−64	−29	23	Supramarginal gyrus, inferior parietal gyrus	1661
	52	−29	25	Supramarginal gyrus, inferior parietal gyrus, postcentral gyrus, superior temporal gyrus	1904
	−2	−49	47	Bilaterally precuneus, left middle cingulate gyrus	978
7a	−52	−7	31	Postcentral and precentral gyri	2162
	56	−5	27	Postcentral gyrus, precentral gyrus, Rolandic operculum	1779
8a	−60	−55	25	Middle temporal gyrus, angular gyrus, superior temporal gyrus, supramarginal gyrus	4256
	−54	19	3	Triangular and orbital part of inferior frontal gyrus	376
9a	16	−75	49	Bilaterally precuneus, superior parietal gyrus, left middle cingulate gyrus	3038
10a	−6	−67	27	Bilaterally precuneus, middle and posterior cingulate gyri, cuneus, calcarine sulcus, right superior occipital gyrus	7238
11a	−42	31	21	Triangular and opercular part of inferior frontal gyrus, middle frontal gyrus, precentral gyrus	2803
12a	8	−31	−13	Cerebellum, vermis	1356
13a	16	−49	67	Postcentral gyrus, superior and inferior parietal gyri, precentral gyrus	1551
14a	34	−79	51	Inferior and superior parietal gyri, angular gyrus, middle and superior occipital gyri, precuneus	4019
15a	−34	−91	25	Middle and superior occipital gyri, superior and inferior parietal gyri, precuneus, cuneus, angular gyrus, middle cingulate gyrus	4109
	50	−81	23	Middle and superior occipital gyri, cuneus, angular gyrus	1737
	−28	−41	−13	Fusiform gyrus	154
	32	−41	−11	Fusiform gyrus	117
16a	−52	−65	33	Inferior and superior parietal gyri, angular gyrus	2871
	42	−71	55	Angular gyrus, inferior parietal gyrus	321
	−40	15	47	Middle frontal gyrus	200
	62	−43	7	Middle temporal gyrus	184
17a	−10	−69	−35	Cerebellum	526
18a	−12	−91	31	Bilaterally cuneus, superior occipital gyrus, precuneus, calcarine sulcus	2988
19a	−38	−11	55	Postcentral gyrus, precentral gyrus, superior parietal gyrus, superior frontal gyrus	2248
20a	−26	53	37	Middle and superior frontal gyri	2932
	34	53	37	Middle frontal gyrus	512
21a	18	−77	5	Bilaterally calcarine sulcus, lingual gyrus, cuneus, right superior occipital gyrus	4368
22a	42	−91	9	Bilaterally middle and superior occipital gyrus, cuneus, calcarine sulcus, right middle temporal gyrus and inferior occipital gyrus	4619
23a	−6	61	35	Bilaterally medial part of superior frontal gyrus, superior frontal gyrus, right middle frontal gyrus	4495
	−6	−59	31	Left precuneus	102
24a	−24	−97	15	Middle, inferior and superior occipital gyri, fusiform gyrus, lingual gyrus, cerebellum, calcarine sulcus, cuneus	4501

N refers to the number of voxels in each cluster. Anatomical labeling is based on the group data, and was performed with the Automated Anatomical Labeling (AAL) tool. Labels are listed if a cluster extended ≥100 voxels into the AAL defined area. Threshold $t > 8.62$, FWE-corrected $p < 0.05$, and cluster size > 100 voxels.

and while the subjects listened to the audio drama. To allow a comparison not only between the conditions but also between the groups, Fig. 3 shows separately for the blind and sighted groups the resting-state networks IC1r, IC2r, and IC25r and the corresponding audio-drama data networks IC1a, IC3a, and IC24a. Additionally, for these networks, the unthresholded spatial maps for each subject are presented in Fig. S3.

Functional network connectivity

Assessment of functional network connectivity in the blind subjects showed that the resting-state network IC1r correlated significantly with networks IC12r and IC22r, network IC2r correlated with IC3r, and network IC25r correlated with IC12r, IC21r, and IC23r; see Table S1 for details and Table 2 for anatomical labels. Audio-drama network IC1a correlated significantly with IC16a and IC23a, network IC3a correlated with IC7a, and network IC24a correlated with IC4a, IC5a, IC15a, and IC21a; see Table S2 for details and Table 3 for anatomical labels.

In the sighted subjects, the resting-state network IC1r correlated significantly with network IC12r, network IC2r correlated with IC3r and IC23r, and network IC25r correlated with IC5r; see Table S3 for details and Table 2 for anatomical labels. Audio-drama network IC1a correlated significantly with IC6a, IC16a and IC23a, network IC3a correlated with IC2a, IC7a, and IC16a, and network IC24a correlated with IC18a and IC21a; see Table S4 for details and Table 3 for anatomical labels.

The resting-state data showed no significant differences in functional network connectivity between the groups. In the audio-drama data, functional network connectivity was stronger in the blind than sighted subjects between IC24a and IC11a (Bonferroni corrected $p = 0.0035$, $r_{blind} = 0.35$, $r_{sighted} = -0.17$) and between IC24a and IC15a ($p = 0.033$, $r_{blind} = 0.38$, $r_{sighted} = 0.010$). IC11a encompassed the triangular and opercular part of the inferior frontal gyrus in the left hemisphere and extended to the left middle frontal gyrus and precentral gyrus. IC15a encompassed mainly the middle and superior occipital gyrus, cuneus, and angular gyrus bilaterally, see Table 3 for details.

Discussion

During rest, three brain networks (a parietal network, an auditory network, and a tactile network) were spatially more variable and a visual network less variable in the blind than in the sighted subjects. During audio drama, four networks (a parietal network, two auditory networks, and a visual network) were more variable and one visual network less variable in the blind compared with the sighted subjects. Thus, in both conditions, a parietal network and an auditory network were more variable and a visual network less variable in the blind than sighted subjects.

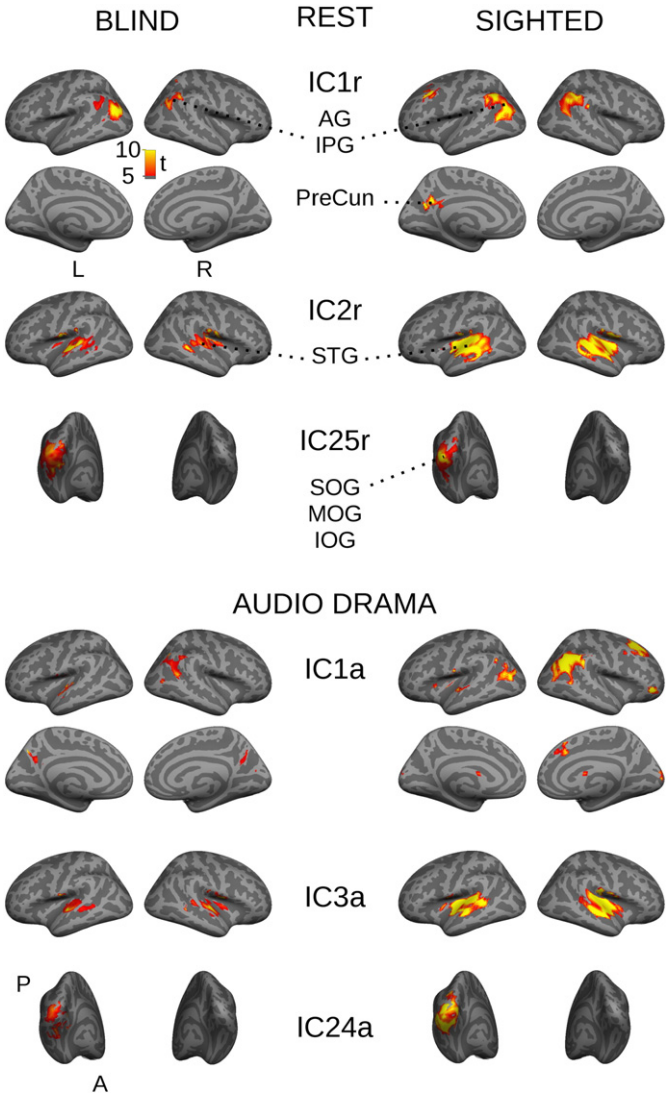

Fig. 3. The functional resting-state and audio-drama networks that were statistically significantly more variable (IC1r and IC1a; IC2r and IC3a), or less variable (IC25r and IC24a), among the blind than sighted subjects during both conditions shown separately for the group of blind and sighted subjects. Two of the networks (IC1r and IC2r during rest and IC1a and IC3a during listening to the audio drama) were significantly more variable in the blind than sighted subjects. One network (IC25r and IC24a) was less variable among the blind than the sighted and encompassed mainly the left superior, middle, and inferior occipital gyri. The mean spatial maps of these networks did not differ between the blind and sighted subjects (two-sample t-test). For illustrative purposes and to allow convenient comparison of the blind and sighted group, the spatial maps are loosely thresholded (uncorrected $p < 0.0005$, cluster size > 300 voxels). The liberal p-value was coupled with a strict cluster threshold to omit spurious clusters. L = left, R = right, A = anterior, P = posterior, AG = angular gyrus, IPG = inferior parietal gyrus, PreCun = precuneus, STG = superior temporal gyrus, SOG = superior occipital gyrus, MOG = middle occipital gyrus, IOG = inferior occipital gyrus.

The parietal networks of the resting-state and audio-drama datasets, (IC1r and IC1a) overlapped in the right inferior parietal gyrus, left precuneus and in the angular gyrus bilaterally, and the auditory networks (IC2r and IC3a) comprised bilaterally the superior temporal and Heschl's gyri, supramarginal and postcentral gyri, Rolandic operculum, and insula. The left-lateralized visual networks (IC25r and IC24a) overlapped in the superior, middle and inferior occipital gyri.

Below our main focus is on the functional network pairs that displayed significant variability differences between the blind and sighted subjects in both the resting-state and audio-drama data. We consider these functional network pairs (IC1r–IC1a, IC2r–IC3a and IC25r–IC24a) spatially rather similar. Employing spatial cross-correlations between these network pairs we found a minimum correlation of $r = 0.42$, which is within the previously reported correlation limits ($r = 0.25$–0.79, mean 0.53) between ICA-derived resting-state and task networks (Smith et al., 2009). Considering that a multitude of factors, such as the number of estimated components, affects the spatial shape and extent of networks between the runs of an ICA (Pamilo et al., 2012), the resting-state and audio-drama networks obtained in the current study corresponded reasonably well with each other. However, as variability is evident even between runs with identical data, variability between different studies is expected. Still, as argued below, our results correspond reasonably well to previous experiments.

Our sample size was small and although statistically significant results based on small samples are worth reporting (Friston, 2012; Lindquist et al., 2013), the low statistical power could conceal true effects and overestimate effect sizes.

Parietal network (IC1r, IC1a)

A bilateral network comprising mainly the angular gyri, and additionally the inferior parietal gyri and precuneus, was spatially more variable in the blind than in the normally-sighted subjects. Angular gyrus is activated in a multitude of tasks, most of which involve language processing (Seghier, 2013), and a functional network encompassing the angular gyrus and precuneus is involved in semantic processing of narratives (Schmithorst et al., 2006). Moreover, the angular gyrus is attributed to language processing also during reading (Segal and Petrides, 2013).

All the blind subjects in the current study read Braille regularly. Therefore, in addition to verbal language processing, the large intra-group spatial variability among the blind in the parietal network could be related to the use of fingers when reading Braille. This notion is supported by the findings that the inferior parietal lobe is involved in Braille reading (Burton et al., 2002; Sadato et al., 1998) and a lesion in the inferior parietal lobule can lead to dysgraphia and finger agnosia (Rusconi et al., 2010).

Auditory network (IC2r, IC3a)

Both during rest and audio drama, an auditory-cortex network, known to react to sounds (Malinen et al., 2007; Schmithorst et al., 2006), was spatially more variable in the blind than in the sighted subjects. The network comprised bilaterally the superior temporal, Heschl's, supramarginal and postcentral gyri, Rolandic operculum, and insula. Early-blind individuals rely strongly on hearing and have a sharper auditory spatial tuning (Röder et al., 1999) and can locate some sounds equally well or better than sighted subjects (Lessard et al., 1998), suggesting compensatory changes in auditory processing (Bavelier and Neville, 2002). However, blind subjects perform poorly in such sound-localization tasks that benefit from calibration of the auditory system by intact vision (Gori et al., 2014; Zwiers et al., 2001). Thus, the blinds' large spatial variability in the auditory network could be related to experience-dependent compensatory changes in auditory cortical areas that varied between the blind subjects during development.

Both human voice and pure tones seem to activate the auditory cortex less intensively in the blind than in the sighted subjects (Gougoux et al., 2009; Watkins et al., 2013). In the light of the current findings, a part of this difference might be explained by increased inter-individual variability in the extent of the auditory network in blind subjects. The current results support the notion that, in the blind, the auditory cortex could be part of an "extended auditory network" reacting less intensively to auditory stimuli (Gougoux et al., 2009).

Visual network (IC25r, IC24a)

Only the visual network—comprising the left superior, middle, and inferior occipital gyri, fusiform and lingual gyri, and the calcarine sulcus—was less variable in the blind than the sighted. Accordingly, the regional homogeneity of local resting-state blood-oxygen-level-dependent signals is increased in the occipital areas of early-blind subjects compared with sighted control subjects (Liu et al., 2011).

We found that the visual network that was spatially less variable in the blind than sighted subjects displayed in the sighted subjects negative functional network connectivity with a frontal language network, but positive connectivity in the blind. This result agrees with earlier studies showing stronger functional connectivity between lateral occipital cortices and frontal language areas in the blind than sighted (Bedny et al., 2011; Watkins et al., 2012). Additionally, the coupling between lateral occipital areas and other visual areas seemed stronger in the blind than sighted subjects. The change in functional connectivity of the lateral occipital area in blind subjects could to some extent affect the extent of the subjects' networks and thus explain the spatial variability differences between the groups. However, as we found no other differences in functional network connectivity between the groups, changes in functional network connectivity in the blind were unlikely the main reason for the spatial variability differences in functional networks between the blind and sighted subjects.

Resting-state brain networks are present already in human infants (Fransson et al., 2007), and the large-scale organization of visual streams could thus develop rather independently of experience (Striem-Amit et al., 2012). On the other hand, it could be driven by the innate retinal waves during fetal development (Goodman and Shatz, 1993). Even though cross-modal recruitment of cortical regions during auditory processing could explain superior auditory performance in blind subjects, the prenatally determined functions are retained in the recruited cortical regions (Lingnau et al., 2014; Renier et al., in press). Thus, we suggest that the primary force of increased inter-individual spatial variability is intra-modal experience-dependent plasticity, while cross-modal plasticity may play a secondary role. Consequently, the relatively small variability of the spatial distribution in this visual network among the blind could be due to the lack of visual information flow in the brain suggesting that the here observed cortical alterations reflect reduced sensory-experience-dependent synaptic pruning (Jiang et al., 2009).

Networks with significant variability differences during only one condition

During rest, a tactile network (IC3r) comprising bilaterally the postcentral gyrus and the right precentral gyrus displayed significantly larger spatial variability in the blind than sighted subjects. The same was true for one visual network (IC4a) during audio-drama listening. Although these results were only seen in one condition and should therefore be interpreted with caution, they could indicate that (i) extensive use of the somatosensory system in the early-blind results in compensatory plasticity in tactile networks (Wang et al., in press) and that (ii) cross-modal recruitment of occipital areas in the early-blind (Renier et al., 2010) plausibly increases inter-subject variability of some, but not all, visual networks.

We observed in sighted subjects larger variability in the lateral visual networks (IC25r, IC24a) than in the network comprising more medial occipital areas (IC4a) (see Fig. 2), analogous to a cytoarchitectonic study in sighted subjects showing larger variability in size and shape in the lateral occipital areas compared with medial occipital areas (Amunts et al., 2000). Whether this result explains why one occipital network (IC25r, IC24a) was more variable in the sighted than the blind subjects, while another occipital network (IC4a) was less variable in the sighted than blind subjects, remains unknown.

Although the cause of the blindness varied among our blind subjects, all subjects could be classified as early-blind. Four subjects were blind from birth and one from 6 months of age, and two had very limited vision before becoming blind at the age of about 3 years. Nonetheless we cannot exclude the possibility that the heterogeneity of our blind subjects could be a major cause for the observed spatial variability. Contrary to this proposition, however, the occipital network comprising visual cortices was more similar among the blind than sighted subjects, rendering the different causes of early-onset blindness an unlikely explanation for increased variability of functional brain networks.

Conclusions

We conclude that networks spatially more variable among the blind than the sighted subjects are related to language processing and hearing, that is to abilities that are expected to compensate for the loss of sight. On the other hand, we observed less variability among the early-blind than the sighted subjects in a left-lateralized visual network that lacks visual information flow in the blind. Based on these observations, we suggest that the degree of spatial variability in a functional network is proportional to the degree of experience-dependent plasticity driven by the sense normally attributed to the network.

Supplementary data to this article can be found online at http://dx.doi.org/10.1016/j.neuroimage.2014.03.058.

Acknowledgments

The study was supported by the Academy of Finland, (grants #131483, #259752, #263800, and #273147) aivoAALTO project of the Aalto University, and European Research Council (Advanced Grant #232946). We thank Marita Kattelus for expert help during fMRI measurements and Ilkka Linnankoski for reviewing the language.

References

Allen, E.A., Erhardt, E.B., Wei, Y., Eichele, T., Calhoun, V.D., 2012. Capturing inter-subject variability with group independent component analysis of fMRI data: a simulation study. NeuroImage 59, 4141–4159.

Amunts, K., Malikovic, A., Mohlberg, H., Schormann, T., Zilles, K., 2000. Brodmann's areas 17 and 18 brought into stereotaxic space—where and how variable? NeuroImage 11, 66–84.

Bavelier, D., Neville, H.J., 2002. Cross-modal plasticity: where and how? Nat. Rev. Neurosci. 3, 443–452.

Bedny, M., Pascual-Leone, A., Dodell-Feder, D., Fedorenko, E., Saxe, R., 2011. Language processing in the occipital cortex of congenitally blind adults. Proc. Natl. Acad. Sci. U. S. A. 108, 4429–4434.

Biswal, B., Yetkin, F.Z., Haughton, V.M., Hyde, J.S., 1995. Functional connectivity in the motor cortex of resting human brain using echo-planar MRI. Magn. Reson. Med. 34, 537–541.

Boldt, R., Malinen, S., Seppä, M., Tikka, P., Savolainen, P., Hari, R., Carlson, S., 2013. Listening to an audio drama activates two processing networks, one for all sounds, another exclusively for speech. PLoS One 8, e64489.

Burton, H., Snyder, A.Z., Conturo, T.E., Akbudak, E., Ollinger, J.M., Raichle, M.E., 2002. Adaptive changes in early and late blind: a fMRI study of Braille reading. J. Neurophysiol. 87, 589–607.

Calhoun, V.D., Adali, T., 2012. Multisubject independent component analysis of fMRI: a decade of intrinsic networks, default mode, and neurodiagnostic discovery. IEEE Rev. Biomed. Eng. 5, 60–73.

Collignon, O., Charbonneau, G., Lassonde, M., Lepore, F., 2009. Early visual deprivation alters multisensory processing in peripersonal space. Neuropsychologia 47, 3236–3243.

Damoiseaux, J.S., Rombouts, S.A., Barkhof, F., Scheltens, P., Stam, C.J., Smith, S.M., Beckmann, C.F., 2006. Consistent resting-state networks across healthy subjects. Proc. Natl. Acad. Sci. U. S. A. 103, 13848–13853.

Di, X., Gohel, S., Kim, E.H., Biswal, B.B., 2013. Task vs. rest-different network configurations between the coactivation and the resting-state brain networks. Front. Hum. Neurosci. 7, 493.

Erhardt, E.B., Rachakonda, S., Bedrick, E.J., Allen, E.A., Adali, T., Calhoun, V.D., 2011. Comparison of multi-subject ICA methods for analysis of fMRI data. Hum. Brain Mapp. 32, 2075–2095.

Fair, D.A., Cohen, A.L., Power, J.D., Dosenbach, N.U., Church, J.A., Miezin, F.M., Schlaggar, B.L., Petersen, S.E., 2009. Functional brain networks develop from a "local to distributed" organization. PLoS Comput. Biol. 5, e1000381.

Fransson, P., Skiöld, B., Horsch, S., Nordell, A., Blennow, M., Lagercrantz, H., Aden, U., 2007. Resting-state networks in the infant brain. Proc. Natl. Acad. Sci. U. S. A. 104, 15531–15536.

Friston, K., 2012. Ten ironic rules for non-statistical reviewers. NeuroImage 61, 1300–1310.

Glahn, D.C., Winkler, A.M., Kochunov, P., Almasy, L., Duggirala, R., Carless, M.A., Curran, J.C., Olvera, R.L., Laird, A.R., Smith, S.M., Beckmann, C.F., Fox, P.T., Blangero, J., 2010. Genetic control over the resting brain. Proc. Natl. Acad. Sci. U. S. A. 107, 1223–1228.
Goldreich, D., Kanics, I.M., 2003. Tactile acuity is enhanced in blindness. J. Neurosci. 23, 3439–3445.
Goodman, C.S., Shatz, C.J., 1993. Developmental mechanisms that generate precise patterns of neuronal connectivity. Cell 72, 77–98 (Suppl.).
Gori, M., Sandini, G., Martinoli, C., Burr, D.C., 2014. Impairment of auditory spatial localization in congenitally blind human subjects. Brain 137, 288–293.
Gougoux, F., Belin, P., Voss, P., Lepore, F., Lassonde, M., Zatorre, R.J., 2009. Voice perception in blind persons: a functional magnetic resonance imaging study. Neuropsychologia 47, 2967–2974.
Gougoux, F., Lepore, F., Lassonde, M., Voss, P., Zatorre, R.J., Belin, P., 2004. Neuropsychology: pitch discrimination in the early blind. Nature 430, 309.
Gougoux, F., Zatorre, R.J., Lassonde, M., Voss, P., Lepore, F., 2005. A functional neuroimaging study of sound localization: visual cortex activity predicts performance in early-blind individuals. PLoS Biol. 3, e27.
Greicius, M.D., Srivastava, G., Reiss, A.L., Menon, V., 2004. Default-mode network activity distinguishes Alzheimer's disease from healthy aging: evidence from functional MRI. Proc. Natl. Acad. Sci. U. S. A. 101, 4637–4642.
Himberg, J., Hyvärinen, A., Esposito, F., 2004. Validating the independent components of neuroimaging time series via clustering and visualization. NeuroImage 22, 1214–1222.
Jafri, M.J., Pearlson, G.D., Stevens, M., Calhoun, V.D., 2008. A method for functional network connectivity among spatially independent resting-state components in schizophrenia. NeuroImage 39, 1666–1681.
Jamadar, S., Powers, N.R., Meda, S.A., Calhoun, V.D., Gelernter, J., Gruen, J.R., Pearlson, G.D., 2013. Genetic influences of resting state fMRI activity in language-related brain regions in healthy controls and schizophrenia patients: a pilot study. Brain Imaging Behav. 7, 15–27.
Jang, J.H., Jung, W.H., Kang, D.H., Byun, M.S., Kwon, S.J., Choi, C.H., Kwon, J.S., 2011. Increased default mode network connectivity associated with meditation. Neurosci. Lett. 487, 358–362.
Jiang, J., Zhu, W., Shi, F., Liu, Y., Li, J., Qin, W., Li, K., Yu, C., Jiang, T., 2009. Thick visual cortex in the early blind. J. Neurosci. 29, 2205–2211.
Joel, S.E., Caffo, B.S., van Zijl, P.C., Pekar, J.J., 2011. On the relationship between seed-based and ICA-based measures of functional connectivity. Magn. Reson. Med. 66, 644–657.
Kim, D., Pearlson, G.D., Kiehl, K.A., Bedrick, E., Demirci, O., Calhoun, V.D., 2008. A method for multi-group inter-participant correlation: abnormal synchrony in patients with schizophrenia during auditory target detection. NeuroImage 39, 1129–1141.
Lee, M.H., Hacker, C.D., Snyder, A.Z., Corbetta, M., Zhang, D., Leuthardt, E.C., Shimony, J.S., 2012. Clustering of resting state networks. PLoS One 7, e40370.
Lee, T.W., Girolami, M., Sejnowski, T.J., 1999. Independent component analysis using an extended infomax algorithm for mixed subgaussian and supergaussian sources. Neural Comput. 11, 417–441.
Lessard, N., Paré, M., Lepore, F., Lassonde, M., 1998. Early-blind human subjects localize sound sources better than sighted subjects. Nature 395, 278–280.
Li, Y.O., Adali, T., Calhoun, V.D., 2007. Estimating the number of independent components for functional magnetic resonance imaging data. Hum. Brain Mapp. 28, 1251–1266.
Lindquist, M.A., Caffo, B., Crainiceanu, C., 2013. Ironing out the statistical wrinkles in "ten ironic rules". NeuroImage 81, 499–502.
Lingnau, A., Strnad, L., He, C., Fabbri, S., Han, Z., Bi, Y., Caramazza, A., 2014. Cross-modal plasticity preserves functional specialization in posterior parietal cortex. Cereb. Cortex 24, 541–549.
Liu, C., Liu, Y., Li, W., Wang, D., Jiang, T., Zhang, Y., Yu, C., 2011. Increased regional homogeneity of blood oxygen level-dependent signals in occipital cortex of early blind individuals. Neuroreport 22, 190–194.
Liu, Y., Yu, C., Liang, M., Li, J., Tian, L., Zhou, Y., Qin, W., Li, K., Jiang, T., 2007. Whole brain functional connectivity in the early blind. Brain 130, 2085–2096.
Malinen, S., Hlushchuk, Y., Hari, R., 2007. Towards natural stimulation in fMRI—issues of data analysis. NeuroImage 35, 131–139.
Mueller, S., Wang, D., Fox, M.D., Yeo, B.T., Sepulcre, J., Sabuncu, M.R., Shafee, R., Lu, J., Liu, H., 2013. Individual variability in functional connectivity architecture of the human brain. Neuron 77, 586–595.
Pamilo, S., Malinen, S., Hlushchuk, Y., Seppä, M., Tikka, P., Hari, R., 2012. Functional subdivision of group-ICA results of fMRI data collected during cinema viewing. PLoS One 7, e42000.
Pascual-Leone, A., Amedi, A., Fregni, F., Merabet, L.B., 2005. The plastic human brain cortex. Annu. Rev. Neurosci. 28, 377–401.
Raichle, M.E., MacLeod, A.M., Snyder, A.Z., Powers, W.J., Gusnard, D.A., Shulman, G.L., 2001. A default mode of brain function. Proc. Natl. Acad. Sci. U. S. A. 98, 676–682.
Renier, L., De Volder, A.G., Rauschecker, J.P., 2013. Cortical plasticity and preserved function in early blindness. Neurosci. Biobehav. Rev. http://dx.doi.org/10.1016/j.neubiorev.2013.01.025 (in press).
Renier, L.A., Anurova, I., De Volder, A.G., Carlson, S., VanMeter, J., Rauschecker, J.P., 2010. Preserved functional specialization for spatial processing in the middle occipital gyrus of the early blind. Neuron 68, 138–148.
Rusconi, E., Pinel, P., Dehaene, S., Kleinschmidt, A., 2010. The enigma of Gerstmann's syndrome revisited: a telling tale of the vicissitudes of neuropsychology. Brain 133, 320–332.
Röder, B., Teder-Sälejärvi, W., Sterr, A., Rösler, F., Hillyard, S.A., Neville, H.J., 1999. Improved auditory spatial tuning in blind humans. Nature 400, 162–166.
Sadato, N., Pascual-Leone, A., Grafman, J., Deiber, M.P., Ibañez, V., Hallett, M., 1998. Neural networks for Braille reading by the blind. Brain 121 (Pt 7), 1213–1229.
Satterthwaite, T.D., Wolf, D.H., Ruparel, K., Erus, G., Elliott, M.A., Eickhoff, S.B., Gennatas, E. D., Jackson, C., Prabhakaran, K., Smith, A., Hakonarson, H., Verma, R., Davatzikos, C., Gur, R.E., Gur, R.C., 2013. Heterogeneous impact of motion on fundamental patterns of developmental changes in functional connectivity during youth. NeuroImage 83C, 45–57.
Schmithorst, V.J., Holland, S.K., Plante, E., 2006. Cognitive modules utilized for narrative comprehension in children: a functional magnetic resonance imaging study. NeuroImage 29, 254–266.
Segal, E., Petrides, M., 2013. Functional activation during reading in relation to the sulci of the angular gyrus region. Eur. J. Neurosci. 38, 2793–2801.
Seghier, M.L., 2013. The angular gyrus: multiple functions and multiple subdivisions. Neuroscientist 19, 43–61.
Smith, S.M., Fox, P.T., Miller, K.L., Glahn, D.C., Fox, P.M., Mackay, C.E., Filippini, N., Watkins, K.E., Toro, R., Laird, A.R., Beckmann, C.F., 2009. Correspondence of the brain's functional architecture during activation and rest. Proc. Natl. Acad. Sci. U. S. A. 106, 13040–13045.
Stevens, M.C., Kiehl, K.A., Pearlson, G., Calhoun, V.D., 2007. Functional neural circuits for mental timekeeping. Hum. Brain Mapp. 28, 394–408.
Striem-Amit, E., Dakwar, O., Reich, L., Amedi, A., 2012. The large-scale organization of "visual" streams emerges without visual experience. Cereb. Cortex 22, 1698–1709.
Wan, C.Y., Wood, A.G., Reutens, D.C., Wilson, S.J., 2010. Congenital blindness leads to enhanced vibrotactile perception. Neuropsychologia 48, 631–635.
Wang, D., Qin, W., Liu, Y., Zhang, Y., Jiang, T., Yu, C., 2013. Altered resting-state network connectivity in congenital blind. Hum. Brain Mapp. http://dx.doi.org/10.1002/hbm.22350 (in press).
Watkins, K.E., Cowey, A., Alexander, I., Filippini, N., Kennedy, J.M., Smith, S.M., Ragge, N., Bridge, H., 2012. Language networks in anophthalmia: maintained hierarchy of processing in 'visual' cortex. Brain 135, 1566–1577 (in press).
Watkins, K.E., Shakespeare, T.J., O'Donoghue, M.C., Alexander, I., Ragge, N., Cowey, A., Bridge, H., 2013. Early auditory processing in area V5/MT+ of the congenitally blind brain. J. Neurosci. 33, 18242–18246.
Yu, C., Liu, Y., Li, J., Zhou, Y., Wang, K., Tian, L., Qin, W., Jiang, T., Li, K., 2008. Altered functional connectivity of primary visual cortex in early blindness. Hum. Brain Mapp. 29, 533–543.
Zilles, K., Amunts, K., 2013. Individual variability is not noise. Trends Cogn. Sci. 17, 153–155.
Zwiers, M.P., Van Opstal, A.J., Cruysberg, J.R., 2001. A spatial hearing deficit in early-blind humans. J. Neurosci. 21 (RC142), 141–145.